ENVIRONMENTAL RESEARCH
LETTERS

LETTER • OPEN ACCESS

Skilful seasonal forecasts of wind energy generation in India during the western summer monsoon

To cite this article: James Norman and Amanda C Maycock 2025 *Environ. Res. Lett.* **20** 044036

View the article online for updates and enhancements.

ENVIRONMENTAL RESEARCH
LETTERS

CrossMark

OPEN ACCESS

RECEIVED
4 December 2024

REVISED
20 February 2025

ACCEPTED FOR PUBLICATION
18 March 2025

PUBLISHED
28 March 2025

LETTER

Skilful seasonal forecasts of wind energy generation in India during the western summer monsoon

James Norman* and Amanda C Maycock

School of Earth and Environment, University of Leeds, Leeds, United Kingdom

* Author to whom any correspondence should be addressed.

E-mail: j.e.norman@leeds.ac.uk

Keywords: wind energy, India, seasonal prediction, energy forecasting, Indian summer monsoon

Supplementary material for this article is available online

Abstract

India's ambitious climate goals include a significant role for wind energy, with plans for a nearly threefold expansion of the existing wind fleet within the next decade. At greater levels of wind deployment, the increased likelihood of extended periods of generation surplus and deficit presents a challenge for managing power supply. It is essential to characterise and predict how this energy source performs within India's monsoon climate to ensure the reliable operation of the electricity system. This study demonstrates, for the first time, how large-scale atmospheric variables are related to seasonal wind energy generation anomalies in India during boreal summer. Furthermore, an operational seasonal forecasting system is shown to skilfully predict the atmospheric predictor variables at a lead time of 1–4 months, indicating an ability to forecast summer wind energy generation at the country and regional level in India. The explanatory power of the chosen atmospheric predictor variables remains high under the near-term planned expansion of the Indian wind fleet. These findings demonstrate the potential utility of seasonal forecast information for electricity system management in India.

1. Introduction

Decarbonisation pathways toward ambitious climate goals consistently include rapid and widespread deployment of wind energy technologies [1]. Like many nations, India has pledged a net-zero compliant economic development pathway, in which wind energy is a key source of low carbon electricity. At the time of writing, India's energy targets include reaching 121 GW installed wind capacity by the year 2032, equating to a threefold increase in wind energy generation over 2023 levels [2].

Wind energy generation, hereafter, 'wind generation' is inherently weather-dependent, with the pattern of generation variability a function of the prevailing climate and timescale considered. In the Indian context, wind energy experiences a strong annual cycle [3, 4] and is affected by distinct modes of variability, acting on interannual [5], intraseasonal [6] and diurnal timescales [7]. The variability of Indian wind generation across a range of timescales is greatest in boreal summer [8, 9], coinciding with enhanced surface winds and the frequent passage of low-pressure systems during the Indian summer monsoon (ISM) [10].

Conventionally, operational approaches for managing power networks focus on maintaining the balance of electrical supply and demand in real time. Consequently, numerical weather predictions, spanning minutes to days, are routinely used to provide short-term foresight of generation variability [11]. However, as the likelihood of prolonged periods of generation surplus and deficit increase at higher levels of wind deployment, so too does the need to characterise and anticipate generation variability at longer lead times [12–14].

The potential utility of long-range climate forecasts for the energy sector has long been recognised [15–17], opening the possibility to inform operational measures such as the availability and scheduling of controllable generation and management of energy storage [13]. Seasonal climate forecasts (SCF) are increasingly used in energy sector operations in several regions, guiding decision-making and risk management strategies on weekly-to-monthly forecast horizons [18, 19]. Examples of skilful prediction of energy-relevant meteorological variables on sub-seasonal-to-seasonal timescales are found for the Euro-Atlantic sector [20–23], China [24, 25] and North America [26]. However, less attention has been paid to the potential value of SCF for the Indian electricity system, despite the country hosting the third largest wind fleet globally (∼45 gigawatts—GW) and ambitious plans for near-term expansion [2].

SCF has a long pedigree in South Asia [27], with much attention devoted to forecasts of ISM rainfall (ISMR). Current operational SCF systems, based on dynamical models, demonstrate varying levels of forecast skill in ISMR predictions, generally showing ensemble mean correlation with observed seasonal mean ISMR of between 0.35–0.60 [28–30]. A recently upgraded version of the Indian Meteorological Department forecast system achieves the highest reported forecast skill of ISMR from a dynamical model ($r = 0.63$–0.72 depending on the rainfall dataset used for verification; [30]). At the time of writing, only two studies provide insight into the seasonal forecast skill of energy-relevant variables in India [31, 32]. The earlier of the two assesses four meteorological fields in seven regional subdivisions of India across six operational forecasting models [31]. They find generally modest skill with the European Centre for Medium-Range Weather Forecasts (ECMWF) System 5 performing best for the variables, with a generally higher skill in southern and central regions. The later study considers the seasonal forecasting system used by the National Centre for Medium Range Weather Forecasting (NCMRWF) of India, and demonstrates skillful ensemble mean predictions of surface wind speed during the summer monsoon season over India [32]. However, neither study resolves questions of potential predictability in energy generation itself.

Motivated by these needs, this paper addresses the following objectives: (1) identify climate predictors that are related to seasonal wind generation anomalies during boreal summer in India; and (2) assess the skill of an operational SCF system for capturing the climate predictors at a 1–4 month lead time, thus evaluating the potential to forecast Indian wind generation in summer. The remainder of the paper is laid out as follows: section 2 describes the method used to create a synthetic wind generation dataset for India and seasonal forecasting system used in the analysis; section 3 presents the results of generation variability analysis and seasonal predictions, and section 4 summarises the main findings and wider implications of the results.

2. Data and methods

2.1. Synthetic wind generation timeseries

The short records of observed wind generation in India (just 4–10 years, depending on the region) limits the study of generation variability on interannual timescales. Therefore, a multi-decadal reanalysis-based synthetic wind generation timeseries was constructed using the method described in Norman *et al* [9]. Briefly, the method uses near-surface wind speed data from the ERA5 reanalysis [33] to estimate wind energy generation for all wind farms in India based on installed capacity in the year 2021. A dataset of wind farms in India was compiled from government and industry records (figure 1(a)). The dataset includes information on the turbine model and associated power curve (a functional relationship between tangential wind speed at the turbine's hub height and power output). The simplified power-law model of vertical wind shear within the planetary boundary layer is used to extrapolate wind speeds on fixed vertical levels to the hub height of each turbine [34]. To achieve this, hourly wind shear exponents were computed empirically at each grid cell using 10 m and 100 m wind speed data. A synthesis of hourly wind generation was conducted per wind farm, using the power curve of turbines at each wind farm and wind speed from the nearest reanalysis grid cell, with the appropriate vertical scaling applied.

The resulting generation time series for each wind farm are aggregated to regional and national levels (figure 1(b)) and are expressed as daily capacity factors, which is the ratio of daily generation to maximum attainable generation for installed capacity over 24 h. The generation time series is calibrated against historical records of wind generation [37] using a constant multiplicative adjustment factor applied to wind speeds at all wind farms within respective Indian states. The adjustment factors that minimise mean bias in the synthetic capacity factors compared to the verification data over the period 2017–2021 are found iteratively. The calibrated wind generation synthesis performs well for both the all-India aggregate case (figure 1(c)) and constituent states (see supplementary material section 1, figure A1), showing high correlation with observed daily generation values (all-India r value = 0.98) and low daily mean absolute percentage error (all-India value = 8%). This study focusses on the boreal summer period, specifically, the mean value of synthetic wind capacity factors for June to September inclusive (referred to as JJAS herein). Modest declining trends in the JJAS timeseries of synthetic wind capacity factors for all India and sub-regions were first removed (significant at the 99% level in all regions except the Southern region, using a Mann–Kendal test) before calculating seasonal anomalies.

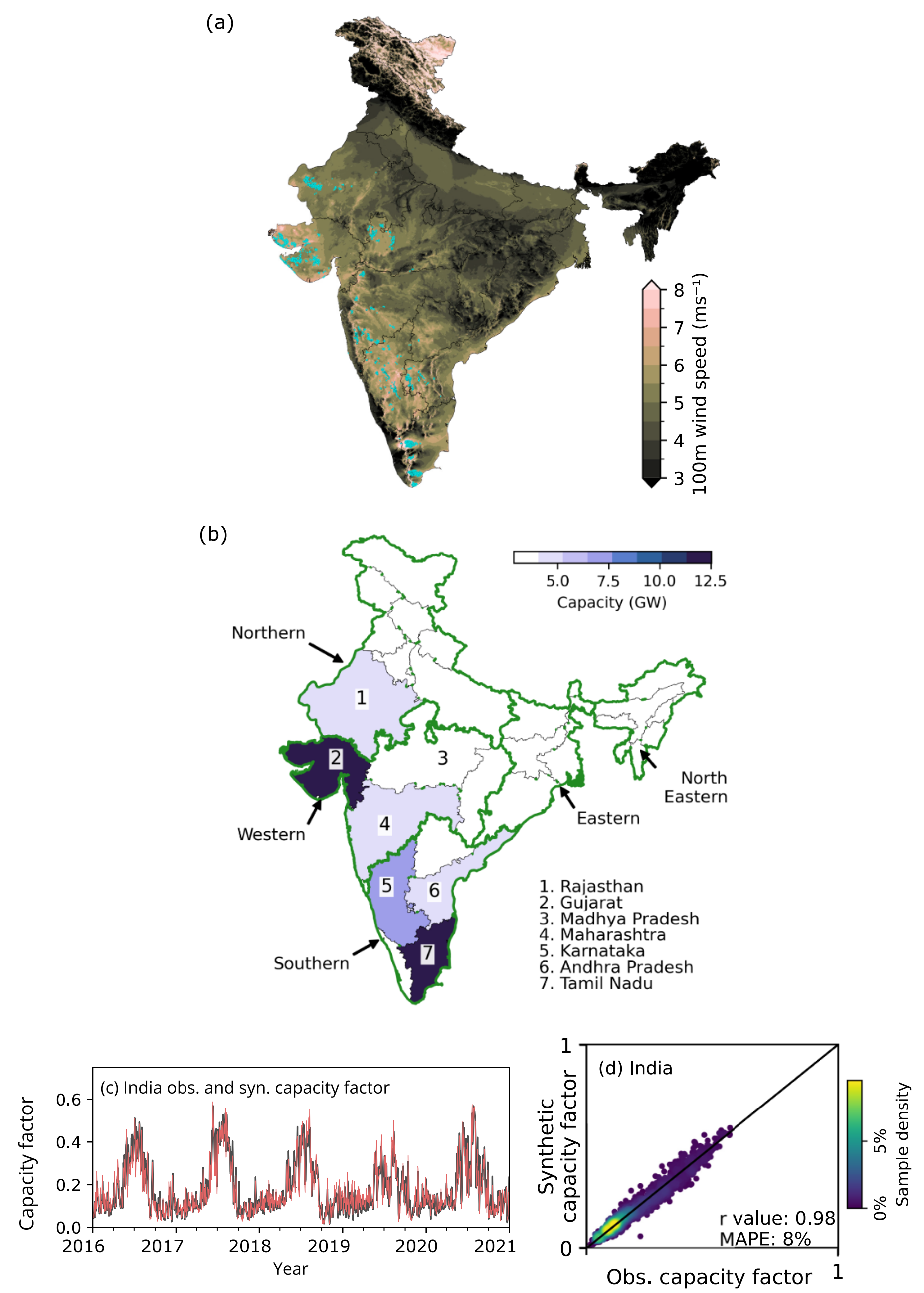

Figure 1. (a) Blue points show wind farm locations in India, using data sources described in Norman *et al* 2024 [9], with shading representing 100 m mean wind speeds (using data from the Global Wind Atlas [35]); (b) five regional electricity grids in India used in this study (green lines) and Indian states shaded by installed wind capacity as of March 2024 [36]; (c) daily wind generation synthesis for all-India during 2016–2021 (red) and equivalent observed values (black); and (d) as in (c) presented as scatter plot.

2.2. Seasonal climate forecasts

This study uses the ECMWF seasonal forecasting system 5 (SEAS5); a global coupled ocean-atmosphere seasonal forecast model that began operational use in 2017 [38, 39]. The atmospheric component of the SEAS5 model has a horizontal resolution of approximately 36 km and 91 vertical levels [39]. This study considers 51-member 41 year-long (1981–2021) hindcast dataset initialised on the 1 May and run for seven months, with model output variables available at a 6 h timestep.

2.3. Wind generation forecasts

Since direct estimates of wind generation in a forecast model are affected by model biases, the predictions use a perfect-prognosis approach that exploits observed statistical relationships between climate predictor variables and the wind generation synthesis dataset [40, 41]. Seasonal forecast skill is then evaluated using the same statistical model, but with predictor variables from the SCF system (e.g. [42–44]). The utility of candidate climate predictors in a seasonal forecasting context depends on the proportion of total generation variance accounted for by the predictors and the forecast skill of the predictor. Accordingly, a predictor variable with high explanatory power is of limited use if it is poorly predicted. Observation-based relationships between climatic indices and JJAS wind capacity factor anomalies are derived using least squares linear regression over the period 1979–2021. The indices are described in section 2.5. Where appropriate, multiple predictors are combined using a multi-linear regression.

The linear regression is first calculated and applied to forecasts using all available reanalysis and hindcast years. A forecast calibration is then undertaken by inflating ensemble variance via a method known as Climate Conserving Recalibration (CCR) [45], and the mean bias removed. Following convention, the calibration and bias correction are undertaken in a cross-validated or leave-one-out set-up, whereby the year being adjusted is excluded from the calculation (i.e. each year is adjusted using information from all other years). This approach mimics an operational setting whereby only past observations inform the empirical relationship utilised in the forecast. Following Doblas-Reyes *et al* [46], Torralba *et al* [26] and Manzanas *et al* [42], the CCR and mean bias correction is implemented as:

$$F^{'}_{n,t} = \rho \frac{\sigma_o}{\mathrm{std}\left(\bar{F}_t\right)} \bar{F}_t + \sqrt{1-\rho^2}\frac{\sigma_o}{\sqrt{\langle \sigma_f^2 \rangle}} \left(F_{n,t} - \bar{F}_t\right) \tag{1}$$

where $F_{n,t}$ and $F^{'}_{n,t}$ denote the original and adjusted forecast for ensemble member n at year t; $\bar{F}_t$ the ensemble mean, σ_o the observed interannual standard deviation, $\langle \sigma_f^2 \rangle$ the mean intra-ensemble variance (i.e. the time mean of ensemble variance per year), and ρ the correlation between the interannual timeseries of observations and the ensemble mean. Essentially, CCR modifies the ensemble spread to achieve the same interannual variance as observations while maintaining the same interannual correlation and forecast ensemble mean (hence 'climate conserving'). Mean bias in the calibrated forecast is removed by calculating anomalies and adding the observed climatology (again in cross-validation mode).

2.4. Forecast verification methods

Forecast skill is measured using the Pearson correlation coefficient between the ensemble mean seasonal mean prediction and the observation-based validation data. Three probabilistic skill scores are also employed: the Brier score, the Ranked Probability Score (RPS), and the Continuous RPS (CRPS) [47]. Following convention, accuracy measures are defined using tercile forecast categories of below normal, normal and above normal, which are defined relative to observed and forecast climatological frequencies [48]. Therefore, Brier score and RPS are insensitive to forecast bias, as tercile categories are defined relative to the modelled climate (while the CPRS is sensitive to forecast bias). Skill scores for the three measures are defined as the relative improvement compared to a climatological reference forecast, with values ranging between -1 and 1, where 1 indicates perfect skill. Additional components of overall forecast quality, namely reliability, sharpness and resolution are assessed using an attributes diagram, with accompanying methodological description in the supplementary material section 2). Statistically significant trends[1] were found in 10 m wind fields. For consistency with the reanalysis-based wind generation synthetic data, the SCF 10 m winds were first detrended by removing the linear least-square regression fit. Other variables show no clear linear trends across the study region, so detrending was not conducted.

2.5. Large-scale climate indices

Following Wang and Fan [49], an index for the ISM strength (ISMi) is defined as the difference between the area average 850 hPa zonal wind (u850) over Southern (40°–80° E, 10°–40° N) and Northern (40°–80° E, 10°–40° N) regions (figure 2(a)). Furthermore, the Western North Pacific index (WNPi) is defined as the difference between area average u850 over Southern (7.5°–17.5° N, 100°–140° E) and Northern (20°–30° N, 105°–150° E) regions of the West Pacific (figure 2(a)). Additionally, an ISMR index is used defined as the standardised rainfall anomaly averaged over 18.5°–26.5° N, 71.5°–86.5° E, and a WNP Rainfall (WNPR) index averaged over 110°–160° E; 10°–20° N (see figure 2(b)). Both rainfall indices are calculated using the Multi-Source Weighted-Ensemble Precipitation (MSWEP) dataset [50]; a gauge-adjusted, satellite-derived rainfall product.

2.6. Scenario for 'planned expansion' of wind farms

Finally, an additional wind generation synthesis is constructed to represent a 'planned expansion' scenario for near-term wind expansion up to 2026. Planned wind capacity is added to the existing database of Indian wind farms that runs to 2021 using the following three sources:

(i) Operational wind farms commissioned in the years 2022 and 2023 using data from Global Energy Monitor, an independent research organisation that maintains global inventories of wind installation locations (+4.3 GW) [51].
(ii) Planned and under construction onshore wind capacity detailed in the project inventory of the

[1] Assessed with a Mann–Kendal test, significant at the 95% level.

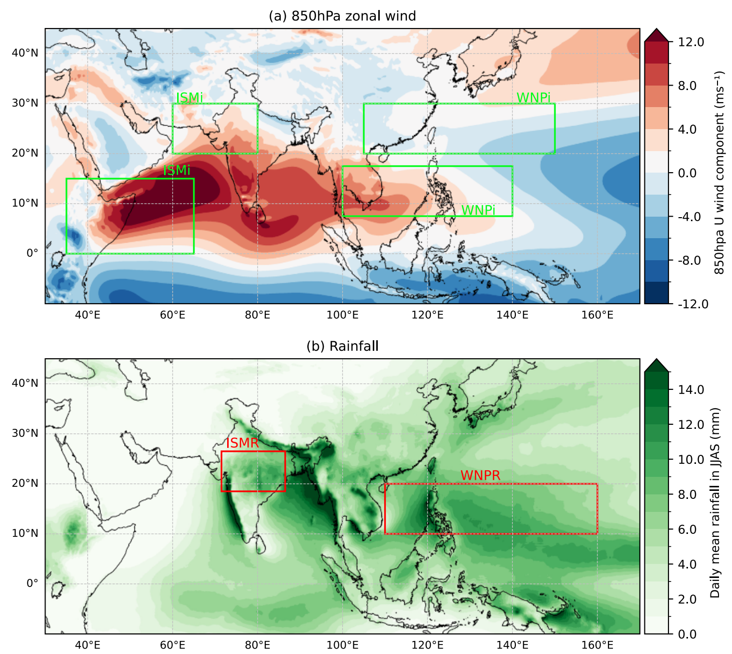

Figure 2. (a) Climatological ERA5 850 hPa zonal wind in JJAS, with green boxes showing used for the ISMi and WNPi indices. (b) Climatological MSWEP daily mean rainfall in JJAS, with red boxes showing the regions used for the ISMR and WNPR indices.

Central Energy Agency of India (+20.1 GW) [52].

(iii) Planned offshore wind capacity to be completed by 2026, following the Ministry of New and Renewable Energy (MNRE) Strategy for Offshore wind (MNRE, 2023)[2].

In total, the 'planned expansion' scenario considers an Indian wind fleet of 81.2 GW, approximately double the capacity in 2021. It is assumed that all additional onshore capacity makes use of a modern turbine model power curve (Suzlon S144 3.15 MW). Offshore capacity makes use of a Siemens Gamesa SG11.0-200 DD 11 MW 120 m, which is a typical offshore model at the time of writing. The 'planned expansion' scenario uses ERA5 winds with no adjustments (as no relevant observational generation data exists for such a calibration).

3. Results

3.1. Observed drivers of seasonal wind generation variability in JJAS

The ISM circulation is prominent in the ERA5 JJAS 850 hPa wind speed climatology, with the greatest wind speeds corresponding with the Somali Jet (figure 3(a)). There is pronounced interannual variability, with the standard deviation reaching ∼35% of the JJAS climatology over central India (figure 3(b)). Figure 3(c) shows the correlation between JJAS wind capacity factor anomalies for all India and JJAS 850 hPa wind speeds across the region. Figures 3(d)–(f) show the same correlation but for sub-regions of the electricity grid system of India, specifically, the Western region (WR; figure 3(d)), Southern region (SR; figure 3(e)), and Northern region (NR; figure 3(f)). All India, Western and Southern regions show similar patterns, with positive correlation across the north Arabian Sea, peninsular India and between the Bay of Bengal and the South China Sea. For Northern region (figure 3(f)), the positive correlation between wind capacity factor anomalies and 850 hPa wind speed is less widespread.

Interestingly, all India wind generation anomalies are negatively correlated with wind speed in the core and southern flank of the Somali Jet, as well as across south-east China. The negative-positive dipole pattern of correlation between the Somali Jet and northern/central India suggests a negative correlation between wind generation and ISMR, as surplus ISMR seasons are associated with an enhanced Somali Jet, increased cross equatorial flow and enhanced easterlies over Northern India [54]. Table 1 summarises the correlation between regional wind generation in JJAS with ISMR and the ISMi index for monsoon strength. Modest negative correlations prevail, suggesting that the intensity of the ISM cannot explain the majority of interannual wind generation variability in JJAS

[2] The strategy details 37 GW in offshore tenders by 2030 Gujarat and Tamil Nadu. The Global Wind Energy Council projects 17.3 GW to be completed by 2026 [53], with capacity split 50/50 between offshore zones in Gujarat (Gulf of Khambhat) and Tamil Nadu (Cape Comorin and Palk Strait).

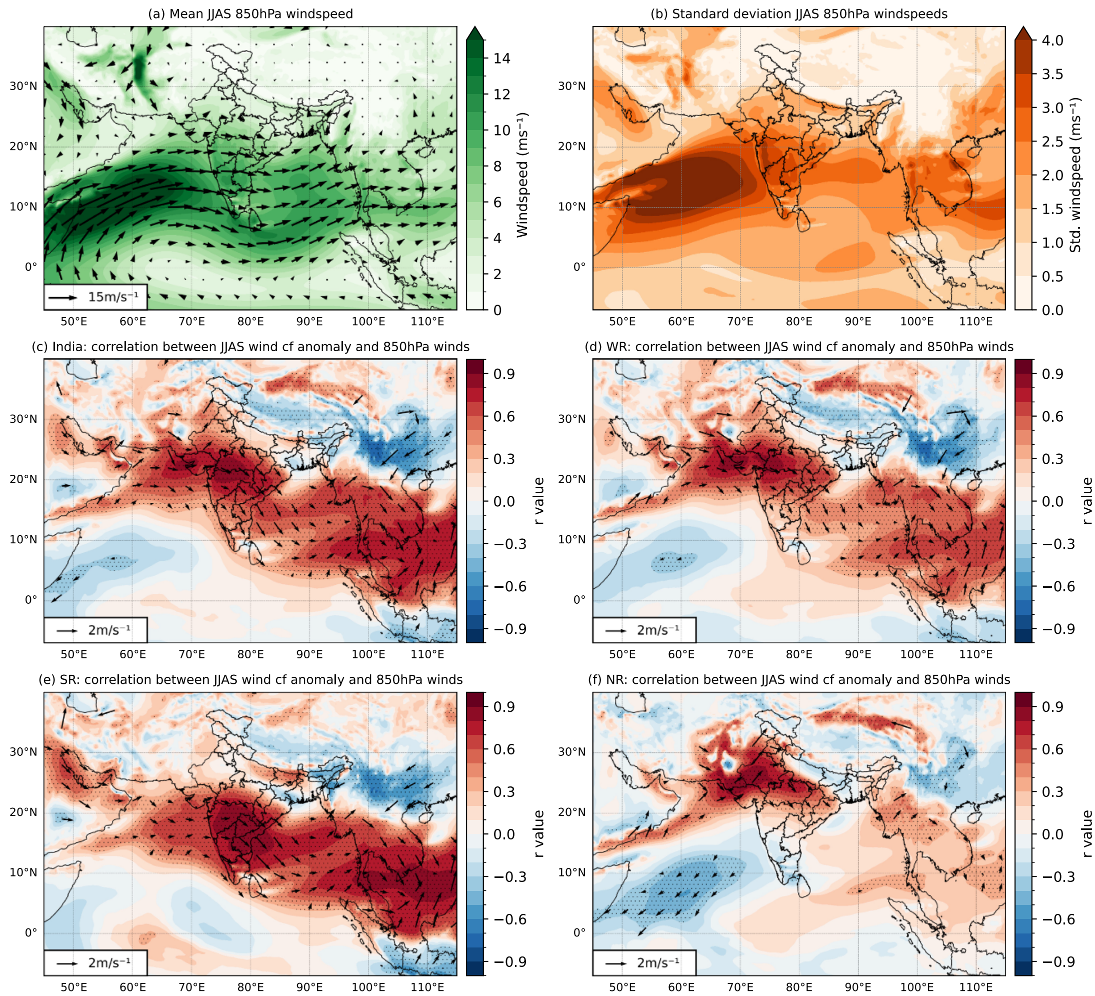

Figure 3. ERA5 JJAS 850 hPa wind speed and direction (a) climatology (1979–2021) and (b) standard deviation. Correlation between JJAS mean wind capacity factor anomalies and 850 hPa winds for (c) all-India, (d) Western region, (e) Southern region and (f) Northern region. Stippling denotes regions significant at 95% confidence level.

Table 1. Interannual Pearson correlation coefficient between regional wind generation anomalies in JJAS and measures of summer monsoon strength, namely ISMR and ISMi. Bold values are significant at the 95% level.

	India	NR	WR	SR
ISMR	**−0.36**	**−0.57**	**−0.41**	−0.11
W-F ISMi	**−0.45**	**−0.65**	**−0.48**	−0.16

(n.b. Northern India represents a minor share of total wind capacity in India −11% in 2021 [36]). The following sections investigate other drivers of interannual wind generation variability in JJAS.

3.2. Climate predictors for India wind generation anomalies in JJAS

To identify the main modes of interannual atmospheric circulation variability over South Asia in boreal summer, an empirical orthogonal function (EOF) analysis of 850 hPa windspeed anomalies average over the JJAS period was conducted over the region (38–125° E; 0–37° N)[3]. Figure 4(a) shows EOF1, which explains 33% of the total interannual variance. The sign convention is that positive loading of EOF1 corresponds to strengthened westerlies over peninsular India, Indo-China, and the Philippine Sea, which converges with the southern flank of a cyclonic anomaly over WNP, representing a strengthening of the regional WNP monsoon [55]. The intensity and westward extent of the WNP monsoon circulation is recognised as the primary mode of interannual atmospheric variability over the South and East Asian regions in JJAS [56–58].

The principal component (PC1) timeseries is positively correlated with the WNPR index ($r = 0.90$) and the WNPi ($r = 0.95$). The correlation pattern in figure 4(a) is similar to the regression map of JJAS wind generation anomalies onto JJAS 850 hPa

[3] The sensitivity of the EOF analysis to the defined geographical extent was tested using different sized domains and yielded similar results (see supplementary material section 3).

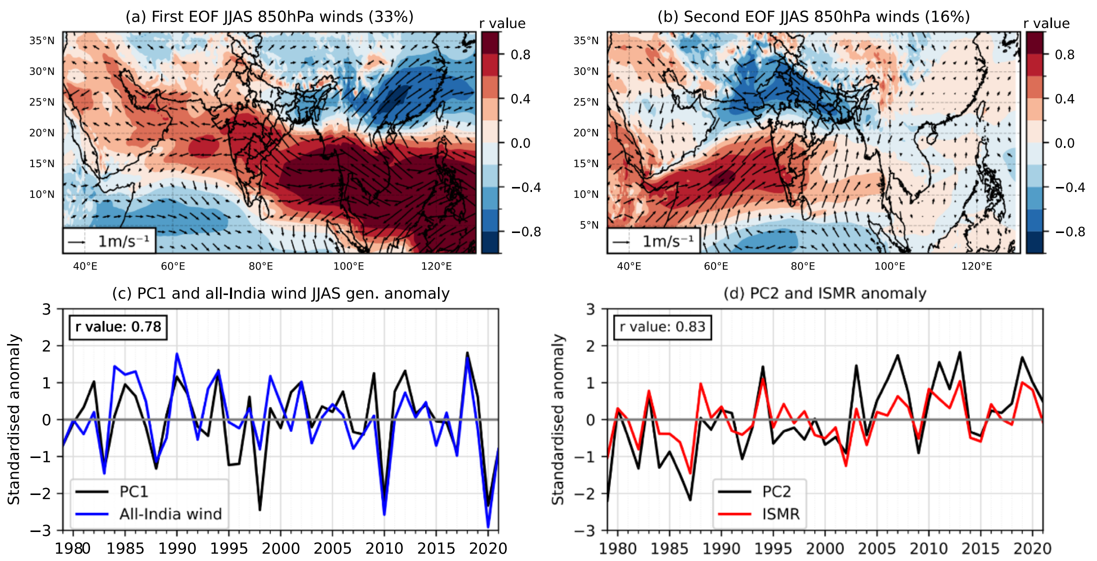

Figure 4. (a) EOF1 and (b) EOF2 of JJAS 850 hPa wind speed anomalies over South Asia (38–125° E; 0–37° N). Vectors denote the wind anomalies for the EOFs and shading denotes the correlation between 850 hPa wind speed and the PC timeseries. (c) Timeseries of PC1 (black) with all-India JJAS wind capacity factor anomalies (blue) and (d) PC2 timeseries (black) with JJAS ISMR anomalies (red).

Table 2. Correlation between wind generation anomalies in JJAS per region and candidate climate predictors. Values in bold are significant at the 95% level.

	All-India	NR	WR	SR
WNP rainfall	**0.68**	**0.33**	**0.56**	**0.71**
WNPi	**0.75**	**0.33**	**0.63**	**0.79**
EOF1	**0.78**	**0.36**	**0.65**	**0.80**
EOF2	−0.19	**−0.50**	−0.24	−0.20
10 m winds	**0.90**	**0.47**	**0.83**	**0.80**

wind speed shown in figures 3(c)–(f). Accordingly, PC1 is highly correlated with India wind generation anomalies (r = 0.78, see figure 4(c) and table 2). Comparably high correlation is also found between wind generation anomalies and the two WNP monsoon indices (WNPR: r = 0.68 and WNPi: 0.75 for all-India, table 2). The strength of these relationships is not as great as between wind generation anomalies and area-weighted 10 m windspeed over India (12°–32° N, 68°–89° E; r = 0.90, referred to as '10 m winds' in table 2), a more directly linked variable. However, the WNPi monsoon still explains more than half the total observed variability of all-India wind generation anomalies.

The second EOF of regional windspeed, which explains 16% of total variance, corresponds to a strengthening of the ISM circulation, with PC2 strongly correlated with the ISMR index (r = 0.83, figure 4(d)). In general, PC2 shows a weak relationship with regional wind generation anomalies, except for a negative association in the Northern region (table 2). Positive loading of EOF2, and the corresponding strengthening of the ISM circulation, is associated with enhanced easterlies in the monsoon trough, which oppose climatological westerlies in the Northern region and reduce wind energy generation.

The statistical relationships between the large-scale climate predictors and Indian wind energy generation identified here can be exploited when using SEAS5 outputs (see section 2.3). The following section evaluates the ensemble mean forecast skill of these three climate predictors.

3.3. Ensemble mean forecast skill of climate predictors

Figure 5(a) shows the grid scale correlation between the SEAS5 ensemble mean and ERA5 10 m windspeed anomalies[4]. Significant positive correlation values are mostly restricted to the subtropics, with northern regions of India showing weak positive correlation and even negative values in the monsoon trough region. The correlation between the area average hindcast ensemble mean and ERA5 10 m windspeed anomalies in the highlighted box in figure 5(a) is r = 0.67. Figure 5(b) shows the correlation between SEAS5 and ERA5 850 hPa windspeed anomalies, which exhibits an overall stronger and more widespread correlation than for 10 m wind speed, particularly in the equatorial Pacific. The correlation between the JJAS WNPi in SEAS5 and ERA5 is 0.75. By comparison, the third climate predictor shows slightly weaker correlation, specifically, between PC1 of the

[4] Calculated by removing observed and model climatology, respectively, not in cross-validation mode.

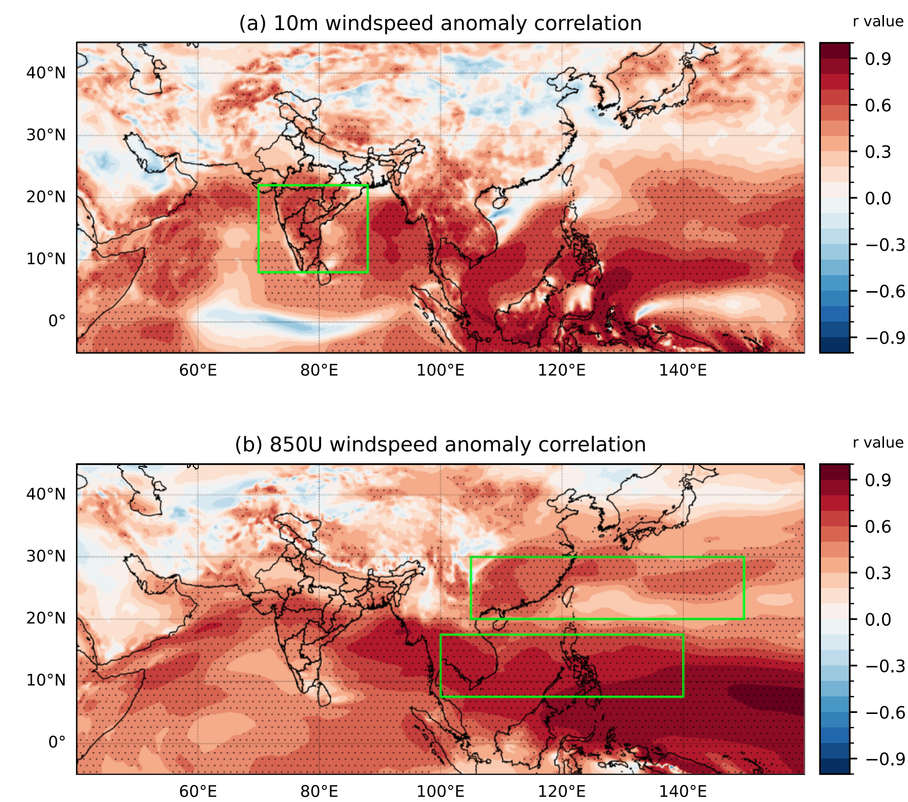

Figure 5. Pearson correlation over 1981–2021 between SEAS5 ensemble mean and ERA5 (a) JJAS 10 m wind speed anomalies and (b) JJAS 850 hPa wind speed anomalies. Green box in (a) denotes 12°–32° N, 68°–89° E. Green boxes in (b) show the regions used to define the WNPi.

EOF decomposition of 850 hPa wind speed anomalies from ERA5 and hindcast ensemble mean[5] ($r = 0.70$).

3.4. Ensemble mean forecast skill of wind generation in India

Now turning to estimates of wind generation, table 3 shows the correlation between predicted and observed JJAS wind generation anomalies at 1–4 months lead time using the observation-based statistical relationships for three predictor variables: WNPi, EOF1 of JJAS u850, and 10 m winds (see table 2). The correlation values are broadly similar across all predictor variables and regions. The Northern region exhibits the lowest skill ($r = 0.45$ with WNPi) and the Southern region the highest ($r = 0.56$ with WNPi). This high correlation reflects the large fraction of variance explained by the WNPi (table 2) and the SEAS5 forecast skill for the WNPi ($r = 0.78$), which is comparable to prediction skill found for other SCF systems (e.g. [59, 60]).

[5] i.e. the EOF decomposition was conducted on each ensemble member before averaging over resulting modes. Alternatively, ensemble members can be projected onto observed modes (i.e. the eigenvectors) and the resulting PCs averaged to gauge similarity in spatiotemporal variability. This approach yields a similar correlation value ($r = 0.71$).

Table 3. Skill of JJAS Indian wind generation forecasts based for three predictor variables. All values are significant at the 95% level. N.B. these predictors are cross-correlated, see main text.

	India	NR	WR	SR
WNPi	0.64	0.45	0.56	0.56
EOF1	0.58	0.36	0.48	0.54
10 m winds	0.62	0.40	0.53	0.56

As all predictors describe similar large-scale atmospheric variability affecting the Indian subcontinent in JJAS, and in many cases are cross-correlated, any combination of the predictors in a multi-linear regression model shows virtually no improvement in skill for wind generation over the single best performing predictor in each sub-region. The only exception is found in the Northern region, where local 10 m winds (averaged over 18°–35° N, 64°–80° E) combined with the WNPi yields a ~12% increase in skill ($r = 0.50$). As mentioned previously, both the ISMi and WNPi are correlated with JJAS wind generation anomalies in this Northern region, so the addition of the 10 m winds as a predictor adds a predictable signal imparted from ISM variability, which is otherwise only partially captured in the WNPi variable.

Splitting the SEAS5 hindcast period considered in this study into early (1981–2001) and late

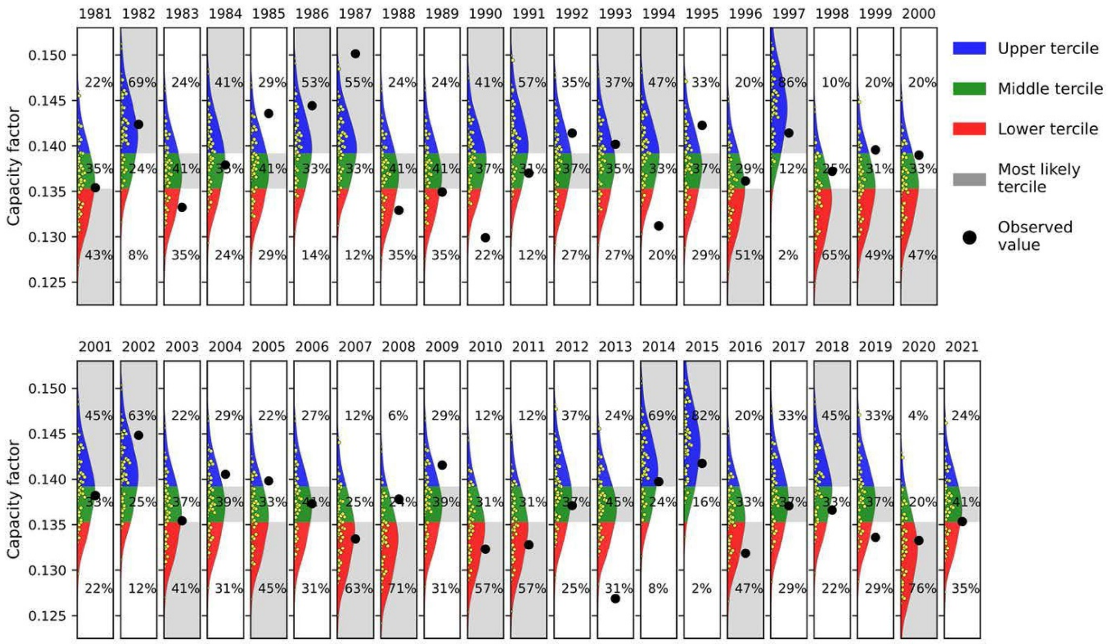

Figure 6. Kernel density estimate of ensemble spread in JJAS wind capacity factors, coloured by tercile, for individual years based on SEAS5 hindcasts. Forecast probabilities per tercile category shown as overlaid text. Individual ensemble members as yellow points and observed values as black points.

Table 4. Forecast quality metrics for 1–4 month lead time JJAS wind generation estimated from the observation-based relationship with the WNPi. Bold (italic) values are significant at the 95% (90%) level based on a bootstrap resampling method. The significance of the r values are based on the 95% level using a two-sided Student's t-test. As described in section 2.3, the forecasts are calibrated using a cross-validation approach, so ensemble mean correlation values are lower than the values listed in table 3.

Wind (JJAS) 1 month lead					
	r value	Brier (low./up./mid.)	CRPSS	RPSS	ROCSS (low./up./mid.)
India	**0.61**	**0.27**/**0.14**/ *0.10*	**0.38**	**0.42**	**0.56**/**0.54**/**0.42**
NR	**0.47**	*0.08*/**0.25**/0.01	**0.35**	**0.45**	**0.62**/**0.38**/−0.07
WR	**0.54**	0.00/**0.22**/0.02	**0.33**	**0.37**	**0.60**/**0.38**/*0.20*
SR	**0.53**	**0.21**/0.00/0.03	**0.32**	**0.35**	**0.45**/**0.56**/*0.20*

(2002–2021) periods reveals higher ensemble mean skill in the late period for all-India generation predictions (full: 0.61, early: 0.48, late: 0.67). The increase in forecast skill in the later hindcast period appears to come from a stronger predictor-predictand relationship (i.e. the relationship between WNPi and wind generation), as the correlation between ensemble mean SEAS5 and observed WNPi values (i.e. predicted and observed WNPi) remains similar (not shown).

3.5. Probabilistic forecast skill of wind generation in India

Using the climate predictor with the highest fraction of total variance explained (i.e. the WNPi), wind capacity factors are estimated for each ensemble member of the SEAS5 hindcasts. The hindcast spread in wind capacity factors for each year are shown in figure 6 for the all-India case. The tercile categories are denoted in colours. The percentages show the fraction of ensemble members in each tercile and black points denote the observed values.

The ensemble members capture the signal of years with strongly negative wind generation anomalies well. The lowest tercile category is correctly predicted by >80% of ensemble members in four of the five lowest generation years (1983, 1988, 1998, 2010, 2020), which are also the years with the five lowest values of the predictor variable. Most of the large negative anomalies coincide with rapid onset of La Nina following transition from El Nino conditions [61].

Although, positive skill is generally found across the forecast verification metrics considered (table 4), insignificant skill is more often found with the discrete measures BSS and RPSS, both of which are more sensitive to ensemble size than r values and continuous measures (e.g. CRPSS) [62]. The Relative Operating Characteristic Skill Score (ROCSS) is also positive for each tercile category, indicating that the number of hits (correct predictions) is greater

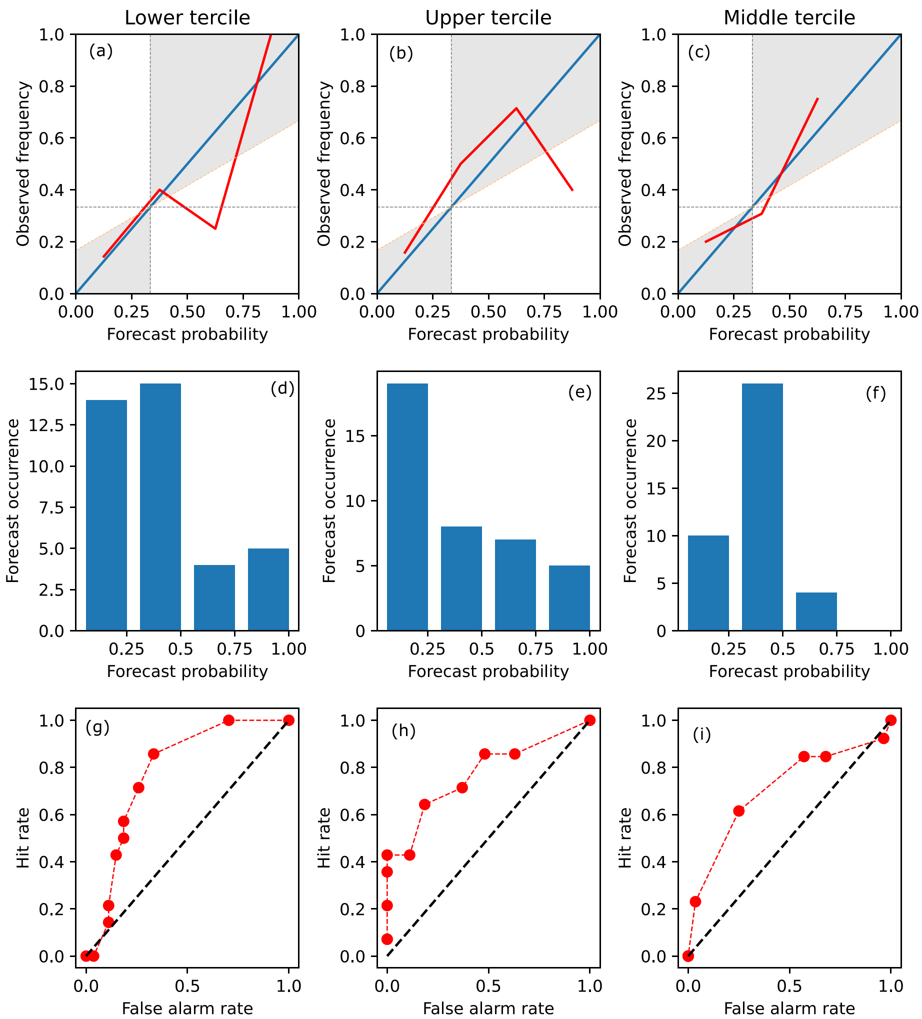

Figure 7. Attributes diagram for 1–4 month lead time JJAS wind capacity factor forecasts based on SEAS5 estimated from the observation-based relationship with the WNPi. (a)–(c) shows the reliability diagram, (d)–(f) shows the sharpness diagrams, and (g)–(i) shows the Relative Operative Characteristic plots, all for lower, upper and middle tercile categories, respectively (see supplementary material section 2 for further details of attributes diagram).

than the number of false alarms (incorrectly predicted non-occurrences) across a range of probability thresholds.

All skill metrics are to some extent sensitive to sample size, though this is particularly the case for assessments of forecast reliability and sharpness [48]. The aggregated wind capacity factor evaluated here provides just one value per hindcast year, which is a smaller effective sample size than for a gridpoint assessment, where events can be pooled across all grid cells within a region. While acknowledging this caveat, the attributes diagram shown in figure 7 suggests the forecasts are reliable and sample a range of probabilities for at least the upper and lower tercile categories—i.e. the correct shape and generally with positive contributions to skill.

3.6. Relevance of climate predictors in expanded wind fleet

The installed capacity of wind power in India is expected to grow significantly in the coming years, expanding into greenfield sites and using modern turbine designs. Different technical parameters of modern turbine designs have been shown to affect wind generation performances and present an additional factor to consider as the wind fleet grows [9].

The explanatory power of the chosen climate predictors was tested for a plausible 'planned expansion' scenario for wind power in India that includes an additional 41.4 GW wind capacity, approximately double the total capacity in 2021 (figure 8). This level of capacity expansion is approximately in line with the midpoint of the planning horizon used in the current National Electricity Plan of India, which envisages a tripling of wind capacity to 121 GW by the year 2032.

Table 5 shows the correlation values between the SEAS5 ensemble mean climate predictors (WNPi, u850 EOF1 and 10 m wind speed) and the ERA5 synthetic wind generation anomalies for the existing fleet and for the 'planned expansion' scenario. The correlation values are very similar across all

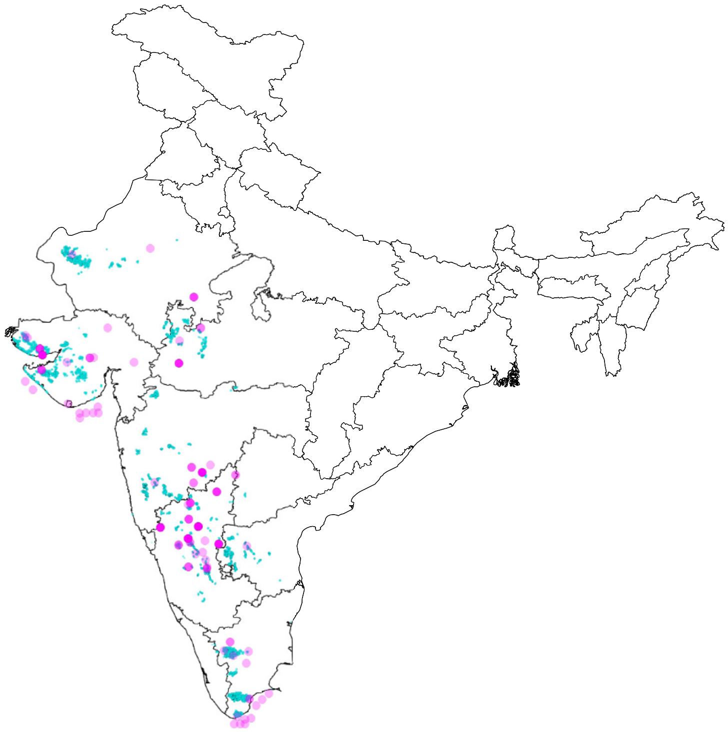

Figure 8. Location of existing wind farms in 2021 (~40 GW, blue points) and additional wind farms considered in the 'expanded scenario' (~41 GW, purple points). Points display spatial information only, with size differentiation for visual clarity.

Table 5. Pearson correlation coefficients between JJAS mean wind capacity factor anomalies per region and the three climate predictors. Values in regular font are for existing wind capacity and underlined font for the 'planned expansion' scenario. All values are significant at the 95% level using a two-sided Student's t-test.

Predictor	All-India	NR	WR	SR	Gujarat Offshore	Tamil Nadu Offshore
W-F WNPi	0.75/<u>0.77</u>	0.33/<u>0.37</u>	0.63/<u>0.66</u>	0.79/<u>0.75</u>	<u>0.61</u>	<u>0.35</u>
u850 EOF1	0.78/<u>0.79</u>	0.36/<u>0.39</u>	0.65/<u>0.66</u>	0.80/<u>0.77</u>	<u>0.61</u>	<u>0.37</u>
10 m winds	0.90/<u>0.92</u>	0.47/<u>0.55</u>	0.83/<u>0.85</u>	0.80/<u>0.78</u>	<u>0.82</u>	<u>0.43</u>

regions in both cases, with very modest increases in the Northern and Western regions. These increases could be due to slightly steeper ramping and/or constant rated power sections of the turbine power curve considered in the additional capacity of the 'planned expansion' scenario. Also, a greater degree of spatial smoothing occurs in the 'planned expansion' scenario, likely causing very slight increases in correlation values for respective regions. Correlation values for individual offshore zones are slightly less than the regional aggregates, likely due to the large concentration of capacity (~8.5 GW) over relatively small areas. However, the generally high correlation across regions show that generation anomalies averaged over the summer season for near-term wind development in India remain well-described by the previously identified predictor variables.

4. Discussion and conclusion

This study has investigated large-scale climate predictors that show observed relationships with boreal summer (JJAS) wind energy generation in India. It then tests the ability of the ECMWF System 5 seasonal forecast model to predict wind capacity factors for India. This exposition is believed to be the first such application of SCFs to wind energy generation in India within the academic literature. The seasonal forecasts at 1–4 months lead time show significant positive skill for wind capacity factors in India and regional subdivisions based on their ability to predict the large-scale climatic variables that show observed relationships with India wind generation.

The ensemble mean forecast skill for all-India capacity factors is similar for all three climate predictors trialed, explaining ~40% of interannual variability in all-India wind capacity factors. Modest improvements to forecast skill in Northern India were achieved using local 10 m winds as an additional predictor. The level of forecast skill found in SEAS5 for India wind generation is comparable to seasonal predictions of energy sector impact variables in some other regions, including boreal winter wind energy in Europe [22]; boreal winter gas demand in the UK

[63], boreal summer electricity demand in Italy [64]; and wind speeds over high wind resource zones of China [24, 25].

The study highlights the roles of monsoon circulations in South Asia on anomalous wind generation in India, namely the ISM and WNP monsoon. The predictive skill found in the wind generation forecasts likely arises from the ability of SEAS5 to accurately represent the ISM (e.g. [38]) and WNP monsoon (e.g. [65]) circulations, which, in turn, are strongly linked with accurate seasonal prediction of tropical sea surface temperature anomalies ([38, 66]; see supplementary material section 5).

Linking specific meteorological phenomena to weather-dependent generation can help the targeted improve generation forecasts in several ways (e.g. [67, 68]). Firstly, a physical interpretation can help assess the limits of predictability (e.g. [69, 70]) and pinpoint important processes for future model development. Second, knowledge of the meteorological drivers behind generation variability may help diagnose varying forecast skill, which can arise due to non-stationarities in the climate system, influencing the strength of teleconnections relevant to the prediction ([71]; and evidenced in Results section 3.4). Furthermore, identifying the main climate driver(s) of prediction skill may help elucidate periods within which forecast skill is enhanced, so-called 'windows of opportunity' [72]. The analysis presented here identified the lowest generation seasons for wind following rapid transitions between ENSO phases, specifically in the four seasons where JJAS wind capacity factors fall below one at least standard deviation (2020, 2010, 1983, 1988). The physical reasoning for the large negative anomalies following peak boreal winter El Nino conditions transitioning to La Nina by the following summer stems from a large anticyclonic anomaly that counters the WNP climatological monsoon circulation and downstream climatological westerlies over India [73, 74]. Future work should determine the extent to which ENSO transition events present a window of opportunity to forecast extreme seasonal wind generation anomalies in India.

Further refinements to the research methodology should include additional calibration of the generation synthesis as more historical generation data becomes available. Additional robustness testing would add to the overall confidence in the verification and prediction quality (e.g. use of different reanalysis datasets—see supplementary material section 4). Model diversity in multi-model assessment has been identified as contributing to pooled skill (e.g. [75]). Therefore, evaluation of other SCF systems would be a worthwhile extension of the work. Other downscaling methodologies are also applicable, including the direct association between forecast ensemble mean and impact variables [76], circulation analogues [77, 78] weather generators [79], and various machine learning methods [80, 81]. Furthermore, different bias correction/calibration methods exist for seasonal forecasts (e.g. quantile mapping, ratio of predictable components). Although verification measures across these various bias correction/calibration methods have shown only marginal differences in other regions of South Asia (e.g. [42]).

Despite the promising indications of forecast skill demonstrated in this study, a substantial fraction of interannual wind generation variability remains unexplained. The potential utility of seasonal forecasts should therefore consider the specific application in the energy sector and the capacity for and implications of using probabilistic forecast information [82]. In such real-world applications, numerous contextual factors may shape the relative pros and cons of forecast-influenced contingencies (e.g. prior experience, the level of comprehension of the forecast information and the availability of contingency measures, etc [83, 84]). Further demonstration of actual or potential forecast value within the context of the Indian electricity system will require deeper consideration of operational procedures [85] and direct collaboration with practitioners [86].

Finally, the analysis presented here is conditioned on the standing stock of wind capacity in India as of 2021, with extra consideration given to a plausible 'planned expansion' scenario. India's national climate targets include a three-fold increase in wind energy generation [2]; however, individual Indian states may proceed at different rates. As such, future work should assess the implications of greater capacity with different geographical configurations for potential predictability. The prospects for generation prediction for other renewable energy technologies also warrant further study, particularly solar photovoltaics (PV), with current plans targeting a six-fold increase in solar PV energy generation over 2023 levels by 2032 [2].

Data availability statement

ERA5 reanalysis data were accessed from the Copernicus Climate Data Store. The dataset of Indian wind farms and synthetic generation timeseries per state is from Norman *et al* [87] and is openly available at the following URL/DOI: https://doi.org/10.5518/1418.

All data that support the findings of this study are included within the article (and any supplementary files).

Acknowledgments

James Norman was supported by a NERC Industrial CASE PhD studentship (NE/S007458/1) and additional grant funding provided by the World Energy and Meteorology Council (WEMC). Amanda C Maycock was supported by the H2020 CONSTRAIN project (Grant Agreement No. 820829) and the Leverhulme Trust.

ORCID iDs

James Norman https://orcid.org/0000-0003-0672-0271
Amanda C Maycock https://orcid.org/0000-0002-6614-1127

References

[1] Luderer G *et al* 2022 Impact of declining renewable energy costs on electrification in low-emission scenarios *Nat. Energy* **7** 32–42
[2] PIB 2023 Central electricity authority notifies the national electricity plan for the period of 2022–32 (available at: https://pib.gov.in/PressReleaseIframePage.aspx?PRID=1928750) (Accessed 11 January 2023)
[3] Lu T, Sherman P, Chen X, Chen S, Lu Xi and McElroy M 2020 India's potential for integrating solar and on-and offshore wind power into its energy system *Nat. Commun.* **11** 4750
[4] Hunt K M R and Bloomfield H C 2024 Quantifying renewable energy potential and realized capacity in India: opportunities and challenges *Meteorol. Appl.* **31** e2196
[5] Gao M, Ding Y, Song S, Lu X, Chen X and McElroy M B 2018 Secular decrease of wind power potential in India associated with warming in the Indian Ocean *Sci. Adv.* **4** eaat5256
[6] Dunning C M, Turner A G and Brayshaw D J 2015 The impact of monsoon intraseasonal variability on renewable power generation in India *Environ. Res. Lett.* **10** 064002
[7] Gangopadhyay A, Seshadri A K and Toumi R 2023 Beneficial role of diurnal smoothing for grid integration of wind power *Environ. Res. Lett.* **18** 014022
[8] Gubbala C S, Dodla V B R and Desamsetti S 2021 Assessment of wind energy potential over India using high-resolution global reanalysis data *J. Earth Syst. Sci.* **130** 1–19
[9] Norman J, Maycock A C, Troccoli A and Dessai S 2024 The role of repowering India's ageing wind farms in achieving net-zero ambitions *Environ. Res. Lett.* **19** 034031
[10] Sikka D R and Gadgil S 1980 On the maximum cloud zone and the ITCZ over Indian longitudes during the southwest monsoon *Mon. Weather Rev.* **108** 1840–53
[11] Foley A M, Leahy P G, Marvuglia A and McKeogh E J 2012 Current methods and advances in forecasting of wind power generation *Renew. Energy* **37** 1–8
[12] White C J *et al* 2017 Potential applications of subseasonal-to-seasonal (S2S) predictions *Meteorol. Appl.* **24** 315–25
[13] Troccoli A 2018 *Weather & Climate Services for the Energy Industry* (Springer Nature)
[14] IEA 2020 Innovation landscape brief: advanced forecasting of variable renewable power generation *Technical Report* (International Renewable Energy Agency (IRENA))
[15] WMO 1979 *World Climate Conf.—Declaration and Supporting Documents* (World Meteorological Organization (WMO))
[16] Weiss E B 1982 The value of seasonal climate forecasts in managing energy resources *J. Appl. Meteorol. Climatol.* **21** 510–7
[17] Knox J B, Moses H and MacCracken M C 1985 Summary report of the workshop on the interactions of climate and energy *Bull. Am. Meteorol. Soc.* **66** 174–84
[18] Orlov A, Sillmann J and Vigo I 2020 Better seasonal forecasts for the renewable energy industry *Nat. Energy* **5** 108–10
[19] White C J *et al* 2022 Advances in the application and utility of subseasonal-to-seasonal predictions *Bull. Am. Meteorol. Soc.* **103** E1448–72
[20] García-Morales M B and Dubus L 2007 Forecasting precipitation for hydroelectric power management: how to exploit GCM's seasonal ensemble forecasts *Int. J. Climatol.* **27** 1691–705
[21] Troccoli A 2010 Seasonal climate forecasting *Meteorol. Appl.* **17** 251–68
[22] Clark R T, Bett P E, Thornton H E and Scaife A A 2017 Skilful seasonal predictions for the European energy industry *Environ. Res. Lett.* **12** 024002
[23] Lledó L, Ramon J, Soret A and Doblas-Reyes F-J 2022 Seasonal prediction of renewable energy generation in Europe based on four teleconnection indices *Renew. Energy* **186** 420–30
[24] Bett P E, Thornton H E, Lockwood J F, Scaife A A, Golding N, Hewitt C, Zhu R, Zhang P and Li C 2017 Skill and reliability of seasonal forecasts for the Chinese energy sector *J. Appl. Meteorol. Climatol.* **56** 3099–114
[25] Lockwood J F, Thornton H E, Dunstone N, Scaife A A, Bett P E, Li C and Ren H-L 2019 Skilful seasonal prediction of winter wind speeds in China *Clim. Dyn.* **53** 3937–55
[26] Torralba V, Doblas-Reyes F J, MacLeod D, Christel I and Davis M 2017 Seasonal climate prediction: a new source of information for the management of wind energy resources *J. Appl. Meteorol. Climatol.* **56** 1231–47
[27] Blanford H F 1884 II. On the connexion of the Himalaya snowfall with dry winds and seasons of drought in India *Proc. R. Soc. Lond.* **37** 3–22
[28] Rajeevan M, Unnikrishnan C K and Preethi B 2012 Evaluation of the ensembles multi-model seasonal forecasts of Indian summer monsoon variability *Clim. Dyn.* **38** 2257–74
[29] Chevuturi A, Turner A G, Johnson S, Weisheimer A, Shonk J K P, Stockdale T N and Senan R 2021 Forecast skill of the Indian monsoon and its onset in the ECMWF seasonal forecasting system 5 (SEAS5) *Clim. Dyn.* **56** 2941–57
[30] Jain D, Rao S, Dandi R, Pillai P, Srivastava A, Pradhan M and Gangadharan K V 2024 Monsoon mission coupled forecast system version 2.0: model description and Indian monsoon simulations *Geosci. Model Dev. Discuss.* **17** 1–29
[31] Das A and Roy S B 2021 Evaluation of subseasonal to seasonal forecasts over India for renewable energy applications *Adv. Geosci.* **56** 89–96
[32] Kumar S, Singh P, Gupta A, Ashrit R, Mishra A K and Rai S 2025 Wind power forecasting over India: value-addition to a coupled model seasonal forecasts *Clean Energy* **9** 37–51
[33] Hersbach H *et al* 2020 The ERA5 global reanalysis *Q. J. R. Meteorol. Soc.* **146** 1999–2049
[34] Schallenberg-Rodriguez J 2013 A methodological review to estimate techno-economical wind energy production *Renew. Sustain. Energy Rev.* **21** 272–87
[35] Global Wind Atlas 2024 Global Wind Atlas (available at: https://globalwindatlas.info/en) (Accessed 14 January 2023)
[36] Ministry of New and Renewable Energy 2022 State-wise installed capacity of renewable power (available at: https://mnre.gov.in/physical-progress/) (Accessed 14 April 2024)
[37] Grid India 2024 Daily power report (available at: https://report.grid-india.in/index.php?p=Daily+Report%2FPSP+Report) (Accessed 9 August 2023)
[38] Johnson S J *et al* 2019 SEAS5: the new ECMWF seasonal forecast system *Geosci. Model Dev.* **12** 1087–117
[39] ECMWF 2021 *SEAS5 User Guide Version 1.2* (European Centre for Medium-Range Weather Forecasts)
[40] Von Storch H, Zorita E and Cubasch U 1993 Downscaling of global climate change estimates to regional scales: an application to Iberian rainfall in wintertime *J. Clim.* **6** 1161–71

[41] Gutiérrez J M, San-Martín D, Brands S, Manzanas R and Herrera S 2013 Reassessing statistical downscaling techniques for their robust application under climate change conditions *J. Clim.* **26** 171–88

[42] Manzanas R, Gutiérrez J M, Bhend J, Hemri S, Doblas-Reyes F J, Torralba V, Penabad E and Brookshaw A 2019 Bias adjustment and ensemble recalibration methods for seasonal forecasting: a comprehensive intercomparison using the C3S dataset *Clim. Dyn.* **53** 1287–305

[43] Baker L H, Shaffrey L C and Scaife A A 2018 Improved seasonal prediction of UK regional precipitation using atmospheric circulation *Int. J. Climatol.* **38** e437–53

[44] Ramon J, Lledó L, Bretonnière P-A, Samsó M and Doblas-Reyes F J 2021 A perfect prognosis downscaling methodology for seasonal prediction of local-scale wind speeds *Environ. Res. Lett.* **16** 054010

[45] Weigel A P, Liniger M A and Appenzeller C 2009 Seasonal ensemble forecasts: are recalibrated single models better than multimodels? *Mon. Weather Rev.* **137** 1460–79

[46] Doblas-Reyes F J, Hagedorn R and Palmer T N 2005 The rationale behind the success of multi-model ensembles in seasonal forecasting—II. Calibration and combination *Tellus* A **57** 234–52

[47] Jolliffe I T and Stephenson D B 2012 *Forecast Verification: A Practitioner's Guide in Atmospheric Science* (Wiley)

[48] Wilks D S 2011 *Statistical Methods in the Atmospheric Sciences* vol 100 (Academic)

[49] Wang B and Fan Z 1999 Choice of South Asian summer monsoon indices *Bull. Am. Meteorol. Soc.* **80** 629–38

[50] Beck H E, Wood E F, Pan M, Fisher C K, Miralles D G, Van Dijk A I J M, McVicar T R and Adler R F 2019 MSWEP V2 global 3-hourly 0.1 precipitation: methodology and quantitative assessment *Bull. Am. Meteorol. Soc.* **100** 473–500

[51] Global Energy Monitor 2023 Global wind power tracker—December 2023 release (available at: https://globalenergymonitor.org/projects/global-wind-power-tracker/download-data/) (Accessed 20 January 2024)

[52] CEA 2024 Report on under construction renewable energy projects (available at: https://cea.nic.in/quarterly-report/?lang=en) (Accessed 20 January 2024)

[53] GWEC 2023 India wind energy market outlook 2023–2027 (available at: https://gwec.net/wp-content/uploads/2023/08/GWEC-India-Outlook-Aug-2023-1.pdf) (Accessed 20 January 2024)

[54] Webster P J, Magana V O, Palmer T N, Shukla J, Tomas R A, Yanai M U and Yasunari T 1998 Monsoons: processes, predictability and the prospects for prediction *J. Geophys. Res. Oceans* **103** 14451–510

[55] Wang B 2006 *The Asian Monsoon* (Springer Science & Business Media)

[56] Wang B, Wu R and Fu X 2000 Pacific–East Asian teleconnection: how does ENSO affect East Asian climate? *J. Clim.* **13** 1517–36

[57] Huang R, Chen J, Wang L and Lin Z 2012 Characteristics, processes and causes of the spatio-temporal variabilities of the East Asian monsoon system *Adv. Atmos. Sci.* **29** 910–42

[58] Xie S-P, Kosaka Y, Du Y, Hu K, Chowdary J S and Huang G 2016 Indo-western Pacific Ocean capacitor and coherent climate anomalies in post-ENSO summer: a review *Adv. Atmos. Sci.* **33** 411–32

[59] Li C, Lu R and Dong B 2012 Predictability of the western North Pacific summer climate demonstrated by the coupled models of ENSEMBLES *Clim. Dyn.* **39** 329–46

[60] Zhang D, Martin G M, Rodríguez J M, Ke Z and Chen L 2020 Predictability of the western North Pacific subtropical high associated with different ENSO phases in GLOSEA5 *J. Meteorol. Res.* **34** 926–40

[61] Global Energy Monitor 2023 Global wind power tracker—December 2023 release (available at: www.cpc.ncep.noaa.gov/products/precip/CWlink/MJO/enso.shtml#history) (Accessed 11 August 2023)

[62] Weigel A P, Liniger M A and Appenzeller C 2007 The discrete Brier and ranked probability skill scores *Mon. Weather Rev.* **135** 118–24

[63] Thornton H E, Scaife A A, Hoskins B J, Brayshaw D J, Smith D M, Dunstone N, Stringer N and Bett P E 2019 Skilful seasonal prediction of winter gas demand *Environ. Res. Lett.* **14** 024009

[64] De Felice M, Alessandri A and Catalano F 2015 Seasonal climate forecasts for medium-term electricity demand forecasting *Appl. Energy* **137** 435–44

[65] Li C, Lu R and Chen G 2017 Promising prediction of the monsoon trough and its implication for tropical cyclone activity over the western North Pacific *Environ. Res. Lett.* **12** 074027

[66] Goddard L M, Mason S J, Zebiak S E, Ropelewski C F, Basher R and Cane M A 2001 Current approaches to season-to-interannual climate prediction *Int. J. Climatol.* **21** 1111–52

[67] Brayshaw D J, Troccoli A, Fordham R and Methven J 2011 The impact of large scale atmospheric circulation patterns on wind power generation and its potential predictability: a case study over the UK *Renew. Energy* **36** 2087–96

[68] Beerli R, Wernli H and Grams C M 2017 Does the lower stratosphere provide predictability for month-ahead wind electricity generation in Europe? *Q. J. R. Meteorol. Soc.* **143** 3025–36

[69] Wang B, Lee J-Y and Xiang B 2015 Asian summer monsoon rainfall predictability: a predictable mode analysis *Clim. Dyn.* **44** 61–74

[70] Saha S K, Hazra A, Pokhrel S, Chaudhari H S, Sujith K, Rai A, Rahaman H and Goswami B N 2019 Unraveling the mystery of Indian summer monsoon prediction: improved estimate of predictability limit *J. Geophys. Res. Atmos.* **124** 1962–74

[71] Wang B, Xiang B, Li J, Webster P J, Rajeevan M N, Liu J and Ha K-J 2015 Rethinking Indian monsoon rainfall prediction in the context of recent global warming *Nat. Commun.* **6** 7154

[72] Mariotti A *et al* 2020 Windows of opportunity for skillful forecasts subseasonal to seasonal and beyond *Bull. Am. Meteorol. Soc.* **101** E608–25

[73] Yang J, Liu Q, Xie S-P, Liu Z and Wu L 2007 Impact of the Indian Ocean SST basin mode on the Asian summer monsoon *Geophys. Res. Lett.* **34** L02708

[74] Wang B, Xiang B and Lee J-Y 2013 Subtropical high predictability establishes a promising way for monsoon and tropical storm predictions *Proc. Natl Acad. Sci.* **110** 2718–22

[75] Alessandri A, De Felice M, Catalano F, Lee J-Y, Wang B, Lee D Y, Yoo J-H and Weisheimer A 2018 Grand European and Asian-Pacific multi-model seasonal forecasts: maximization of skill and of potential economical value to end-users *Clim. Dyn.* **50** 2719–38

[76] Bett P E, Thornton H E, Troccoli A, De Felice M, Suckling E, Dubus L, Saint-Drenan Y-M and Brayshaw D J 2022 A simplified seasonal forecasting strategy, applied to wind and solar power in Europe *Clim. Serv.* **27** 100318

[77] Lorenz E N 1969 Atmospheric predictability as revealed by naturally occurring analogues *J. Atmos. Sci.* **26** 636–46

[78] Zorita E and Von Storch H 1999 The analog method as a simple statistical downscaling technique: comparison with more complicated methods *J. Clim.* **12** 2474–89

[79] Wilby R L and Wigley T M L 1997 Downscaling general circulation model output: a review of methods and limitations *Prog. Phys. Geogr.* **21** 530–48

[80] Vandal T, Kodra E, Ganguly S, Michaelis A, Nemani R and Ganguly A R 2017 DeepSD: generating high resolution climate change projections through single image super-resolution *Proc. 23rd Int. Conf. on Knowledge Discovery and Data Mining* pp 1663–72

[81] Sachindra D A, Ahmed K, Rashid M M, Shahid S and Perera B J C 2018 Statistical downscaling of precipitation using machine learning techniques *Atmos. Res.* **212** 240–58

[82] Soares M B and Dessai S 2016 Barriers and enablers to the use of seasonal climate forecasts amongst organisations in Europe *Clim. Change* **137** 89–103
[83] Lemos M C, Finan T J, Fox R W, Nelson D R and Tucker J 2002 The use of seasonal climate forecasting in policymaking: lessons from Northeast Brazil *Clim. Change* **55** 479–507
[84] Dilling L and Lemos M C 2011 Creating usable science: opportunities and constraints for climate knowledge use and their implications for science policy *Glob. Environ. Change* **21** 680–9
[85] Vincent K, Daly M, Scannell C and Leathes B 2018 What can climate services learn from theory and practice of co-production? *Clim. Serv.* **12** 48–58
[86] Kirchhoff C J, Lemos M C and Dessai S 2013 Actionable knowledge for environmental decision making: broadening the usability of climate science *Annu. Rev. Environ. Resour.* **38** 393–414
[87] Norman J, Maycock A C, Troccoli A and Suraje D 2023 Dataset of Indian wind farms and synthetic wind generation timeseries per Indian state University of Leeds [Dataset] 10.5518/1418